

# Diagnosing fuel $\rho R$ and $\rho R$ asymmetries in cryogenic deuterium-tritium implosions using charged-particle spectrometry at OMEGA

J. A. Frenje,<sup>1</sup> C. K. Li,<sup>1</sup> F. H. Séguin,<sup>1</sup> D. T. Casey,<sup>1</sup> R. D. Petrasso,<sup>1,a)</sup>  
T. C. Sangster,<sup>2</sup> R. Betti,<sup>2,b)</sup> V. Yu. Glebov,<sup>2</sup> and D. D. Meyerhofer<sup>2,b)</sup>

<sup>1</sup>Plasma Science and Fusion Center, Massachusetts Institute of Technology, Cambridge, Massachusetts 02139, USA

<sup>2</sup>Laboratory for Laser Energetics, University of Rochester, Rochester, New York 14623, USA

(Received 27 January 2009; accepted 23 February 2009; published online 22 April 2009)

Determining fuel areal density ( $\rho R$ ) in moderate- $\rho R$  (100–200 mg/cm<sup>2</sup>) cryogenic deuterium-tritium (DT) implosions is challenging as it requires new spectrometry techniques and analysis methods to be developed. In this paper, we describe a new method for analyzing the spectrum of knock-on deuterons (KO-Ds), elastically scattered by primary DT neutrons, from which a fuel  $\rho R$  can be inferred for values up to  $\sim 200$  mg/cm<sup>2</sup>. This new analysis method, which uses Monte Carlo modeling of a cryogenic DT implosion, improves significantly the previous analysis method in two fundamental ways. First, it is not affected by significant spatial-yield variations, which degrade the diagnosis of the fuel  $\rho R$  (spatial yield variations of about  $\pm 20\%$  are typically observed), and second, it does not break down when the fuel  $\rho R$  exceeds  $\sim 70$  mg/cm<sup>2</sup>. © 2009 American Institute of Physics. [DOI: 10.1063/1.3098540]

## I. INTRODUCTION

Cryogenic deuterium-tritium (DT) capsules are routinely imploded with the OMEGA laser system<sup>1</sup> at the Laboratory for Laser Energetics, University of Rochester. These implosions are hydrodynamically equivalent to the baseline direct-drive ignition design for the National Ignition Facility (NIF) (Ref. 2) to allow for experimental validation of the design prior to the first ignition experiments at the NIF. The design consists of a cryogenic-DT-fuel layer inside a thin spherical ablator,<sup>3</sup> which is compressed quasi-isentropically to minimize the laser energy required to achieve ignition conditions. If the capsule is sufficiently compressed, the high areal density ( $\rho R$ ) of the cryogenic DT fuel can support a propagating thermonuclear burn wave due to local bootstrap heating by the DT-alpha particles. Maximizing  $\rho R$  for a given on-capsule laser energy is therefore very important. Determining  $\rho R$  is important as well for assessing implosion performance during all stages of development from energy scaled cryogenic DT implosions at OMEGA to cryogenic fizzes to ignited implosions at the NIF. Determining fuel  $\rho R$  in moderate- $\rho R$  (100–200 mg/cm<sup>2</sup>) cryogenic DT implosions has been challenging as it requires new spectrometry techniques and analysis methods to be developed. A new type of neutron spectrometer, called magnetic recoil spectrometer (MRS),<sup>4–6</sup> has been built, installed, and calibrated on OMEGA for measurement of primarily the down-scattered DT neutron spectrum, from which  $\rho R$  of the fuel can be directly inferred. Another MRS is currently being developed for diagnosing high- $\rho R$  cryogenic DT-capsule implosions at the NIF.

This paper describes a complementary method for analyzing the detailed spectral shape of knock-on deuterons (KO-Ds), elastically scattered by primary DT neutrons, from which  $\rho R$  can be inferred for values up to  $\sim 200$  mg/cm<sup>2</sup>. This new analysis method, which uses Monte Carlo modeling<sup>7</sup> of a cryogenic DT implosion, improves significantly in two fundamental ways the existing analysis method, which uses a relatively simple implosion model to relate the fuel  $\rho R$  to the KO-D yield in the high-energy peak.<sup>8–10</sup> First, it is not affected by significant spatial-yield variations, which degrade the diagnosis of the fuel  $\rho R$  (spatial yield variations of about  $\pm 20\%$  are typically observed). Second, it does not break down when the fuel  $\rho R$  exceeds  $\sim 70$  mg/cm<sup>2</sup>. Modeling of the actual shape of the KO-D spectrum is therefore a more powerful method than the yield method for diagnosing the fuel  $\rho R$  in cryogenic DT implosions.

This paper is structured as follows. Section II describes the analysis method used to model the KO-D spectrum, from which a  $\rho R$  of the fuel can be inferred for a cryogenic DT implosion. Section III presents the experiments, data analysis, and results, while Sec. IV summarizes the paper.

## II. DIAGNOSING FUEL $\rho R$ IN MODERATE- $\rho R$ CRYOGENIC DT IMPLOSIONS USING KNOCK-ON DEUTERONS

Diagnosing fuel  $\rho R$  in DT-filled CH-capsule implosions has been performed routinely at OMEGA for more than a decade.<sup>8–10</sup> In those experiments, two magnet based charged-particle spectrometers (CPSs) (Ref. 11) have been used to measure the KO-D spectrum in two different directions. With the recent implementation of the MRS, a third measurement of the KO-D spectrum is now possible (the MRS can be operated in a charged-particle mode, which involves removing the conversion foil near the implosion<sup>5</sup> and operating the

<sup>a)</sup>Also Visiting Senior Scientist at Laboratory for Laser Energetics, University of Rochester, Rochester, NY 14623, USA.

<sup>b)</sup>Also at Department of Mechanical Engineering and Department of Physics and Astronomy, University of Rochester, Rochester, NY 14623, USA.

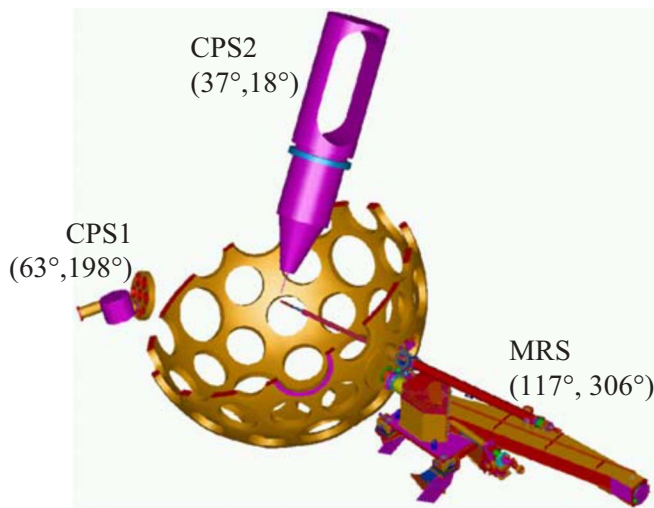


FIG. 1. (Color online) : The MRS and the CPSs (CPS1 and CPS2) on the OMEGA chamber. The line of sight for each diagnostic is illustrated in terms of the polar angle  $\phi$  and azimuthal angle  $\theta$ . These spectrometers are used to simultaneously measure the spectra of elastically scattered deuterons, so-called KO-Ds, from which fuel  $\rho R$  and  $\rho R$  asymmetries in cryogenic DT implosions can be directly inferred. The MRS can operate in either charged-particle or down-scattered neutron mode; the latter mode allows for measurements of the down-scattered neutron spectrum from which  $\rho R$  of the fuel can be inferred as well.

system like a normal CPS). As both  $\rho R$  and  $\rho R$  symmetry are important measures of the performance of a cryogenic DT implosion, the MRS adds significantly to the existing  $\rho R$ -diagnostic suite at OMEGA (Fig. 1).

For a fuel  $\rho R$  around 100 mg/cm<sup>2</sup> about 1% of the primary DT neutrons elastically scatter off the deuterium producing KO-Ds with energies up to 12.5 MeV as expressed by the reaction



At this neutron energy, the differential cross section for the  $n$ -D-elastic scattering in the central-mass system is well known and represents the birth spectrum of the KO-Ds (see Fig. 2). As the KO-Ds pass through the high-density DT fuel they lose energy in proportion to the amount of material they pass through ( $\rho R$ ). A  $\rho R$  value for the portion of the implosion facing a given spectrometer can therefore be determined from the shape of the measured KO-D spectrum by using theoretical formulation of the energy-slowness of deuterons in a plasma.<sup>12</sup> Previous work used a relatively simple model to relate the fuel  $\rho R$  to the yield under the high-energy peak of the KO-D spectrum.<sup>8–10</sup> That model, however, is subject to significant spatial-yield variations that degrade the diagnosis of the fuel  $\rho R$  (spatial yield variations of about  $\pm 20\%$  are typically observed). It also breaks down when the fuel  $\rho R$  exceeds  $\sim 70$  mg/cm<sup>2</sup> because the KO-D spectrum becomes sufficiently distorted by energy-slowness effects that the measurement of the high-energy peak becomes ambiguous; an accurate determination of  $\rho R$  must therefore rely on more sophisticated modeling. Monte Carlo modeling of an implosion, similar to the modeling described in Ref. 7, was instead used to simulate the KO-D spectrum from which a fuel  $\rho R$  can be inferred. This made it possible to use more

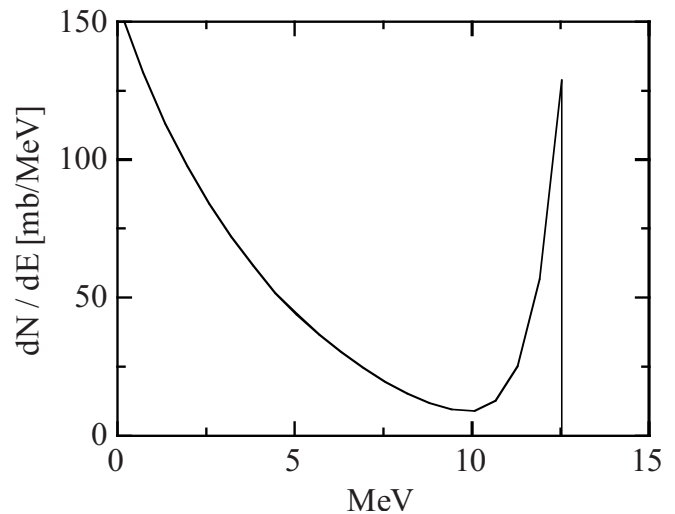


FIG. 2. The birth spectrum of KO-Ds elastically scattered by primary 14.1 MeV neutrons. Due to kinematics, the KO-D high-energy end point is at 12.5 MeV.

realistic temperature and density profiles than those in the hot-spot and uniform models described in Refs. 8–10. From the Monte Carlo modeling, it was established that the shape of the KO-D spectrum depends mainly on fuel  $\rho R$  and that density and electron-temperature profile variations typically predicted in the high-density region play minor roles. This was concluded by studying how the spectral shape varied with varying temperature and density profiles for a fixed  $\rho R$ . The variations were made to still meet the measured burn averaged ion temperature of  $2.0 \pm 0.5$  keV, radius of the high-density region of  $30 \pm 10$   $\mu\text{m}$ , and peak density of 10–160 g/cm<sup>3</sup> (peak density varied less for a fixed  $\rho R$ ). The envelopes (represented by the standard deviation) in which the density and temperature profiles were varied are illustrated in Fig. 3 for a fuel  $\rho R$  of 105 mg/cm<sup>2</sup>. The resulting simulated birth profiles of the primary neutrons and KO-Ds are also shown in Fig. 3. Figure 4 shows how the simulated KO-D spectrum varies with varying  $\rho R$ . The error bars shown in each spectrum represent the effect of varying density and temperature profiles, and as indicated by the error bars, the shape of the KO-D spectrum depends weakly on any profile variations. In contrast, the spectral shape depends strongly on  $\rho R$ . In addition, the modeling was constrained strictly by isobaric conditions at bang time, burn duration, DT-fuel composition, and a steady state during burn. As discussed in Ref. 13, the latter constraint is an adequate approximation for these types of measurements as the time evolution of the fuel  $\rho R$  does not affect significantly the shape of the burn-averaged spectrum, which simplifies the  $\rho R$  interpretation of the measured KO-D spectrum. Multidimensional features could, on the other hand, affect the analysis and interpretation of the KO-D spectrum, as these effects would manifest themselves by slightly smearing out the high-energy peak for low fuel  $\rho R$ s ( $< 100$  mg/cm<sup>2</sup>). For higher  $\rho R$  ( $> 150$  mg/cm<sup>2</sup>), these effects should be less prominent as high-mode nonuniformities would not significantly alter the shape of the KO-D spectrum.

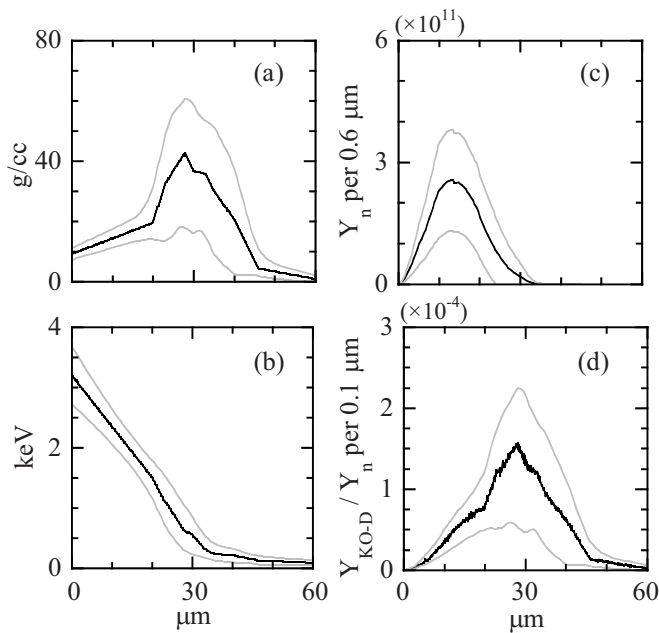


FIG. 3. (a) Density and (b) temperature profiles used in the modeling of a cryogenic DT implosion with a  $\rho R$  of  $105 \text{ mg/cm}^2$ . The black line represents the average, while the gray lines indicate the envelopes (represented by the standard deviation) in which the density and temperature profiles were varied. The variations were made to still meet the measured burn averaged ion temperature of  $2.0 \pm 0.5 \text{ keV}$ , position of the high-density region of  $30 \pm 10 \text{ } \mu\text{m}$ . Resulting birth profiles of the primary neutrons and KO-Ds are shown in (c) and (d). In addition, the modeling was constrained by isobaric conditions at bang time, burn duration, DT-fuel composition, and steady state during burn.

### III. EXPERIMENTS, DATA ANALYSIS, AND RESULTS

The cryogenic DT-capsule implosions discussed in this paper were driven with a laser pulse designed to keep the fuel on an adiabat ( $\alpha$ ) of  $\sim 1-3$ , where  $\alpha$  is the ratio of the internal pressure to the Fermi degenerate pressure.<sup>14</sup> The on-capsule laser energy varied from 12 to 25 kJ, and the laser intensity varied from  $3 \times 10^{14}$  to  $10^{15} \text{ W/cm}^2$ . Full single-beam smoothing was applied during all pulses by using distributed phase plates,<sup>15</sup> polarization smoothing with birefringent wedges,<sup>16</sup> and two-dimensional (2D) single-color cycle, 1 THz smoothing by spectral dispersion.<sup>17</sup> The ablator was typically made of 5–10  $\mu\text{m}$  of deuterated polyethylene (CD), which was permeation filled with an equimolar mixture of DT gas at 1000 atm. At this pressure, the shell and gas were slowly cooled to a few degrees below the DT triple point (19.8 K), typically producing a DT ice layer of thickness of 90–100  $\mu\text{m}$ ,<sup>14</sup> which is thicker than the OMEGA design energy scaled from the baseline direct-drive ignition design for the NIF. The thicker DT ice was chosen to increase the shell stability during the acceleration phase of the implosion. In addition, by tailoring the adiabat in the shell and fuel, the expected imprint perturbation growth for such thick shell is substantially reduced, further improving the implosion performance. Based on one-dimensional (1D) hydrocode simulations,<sup>18</sup> the burn averaged fuel  $\rho R$  is in excess of  $200 \text{ mg/cm}^2$  for these types of implosions.

Figure 5 shows examples of measured and fitted simulated KO-D spectra for four different low-adiabat cryogenic

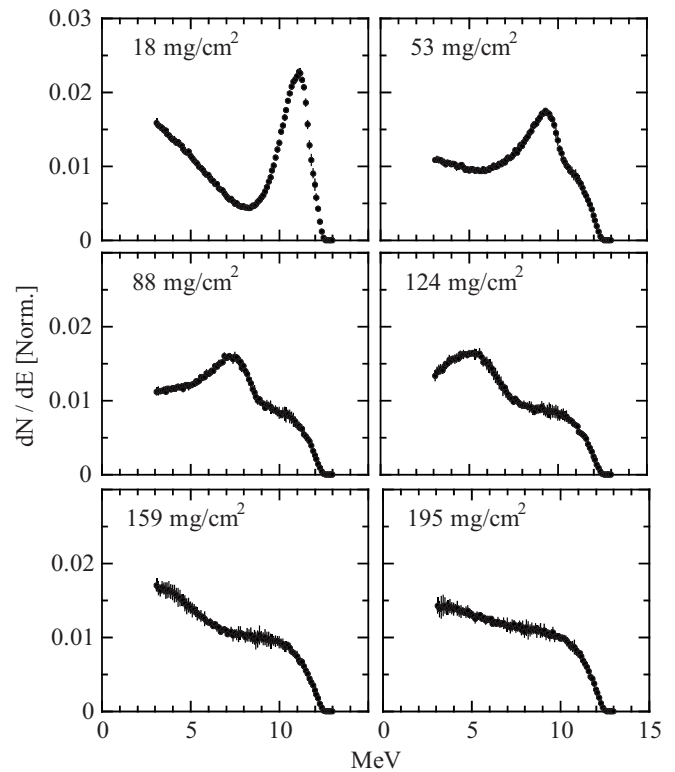


FIG. 4. KO-D spectra for different fuel  $\rho R$ s. The error bars shown in each spectrum represent the effect of varying density and temperature profiles. As illustrated, the shape of the KO-D spectrum depends strongly on  $\rho R$ , while density and temperature profile effects play minor roles as indicated by the error bars. The KO-D spectra are normalized to unity.

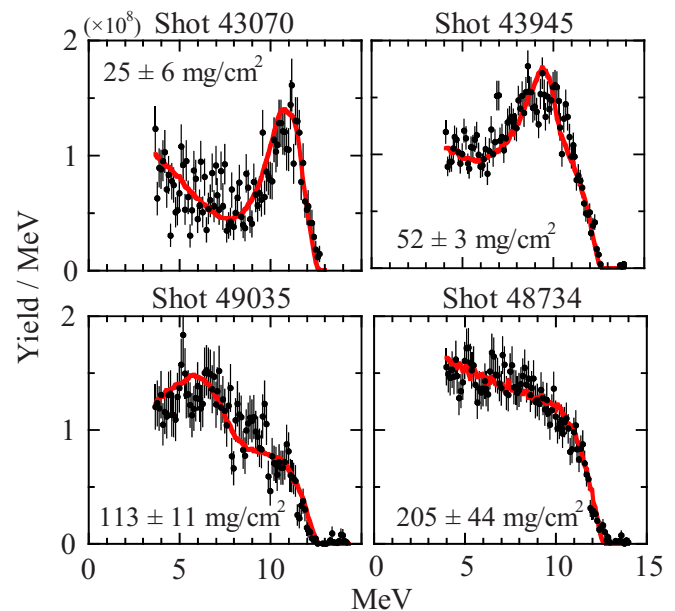


FIG. 5. (Color online) Examples of measured KO-D spectra for four different low-adiabat cryogenic DT implosions. Simulated fits [gray lines (red online)] to the measured spectra are also shown. From the fits, a fuel  $\rho R$  of  $25 \pm 6$ ,  $52 \pm 3$ ,  $113 \pm 11$ , and  $205 \pm 44 \text{ mg/cm}^2$  was determined for shot 43 070, 43 945, 49 035, and 48 734, respectively. The errors of the inferred  $\rho R$  values are due to mainly modeling uncertainties as discussed in Sec. II and statistical uncertainties in the experimental data. See text for more detailed information about these implosions.



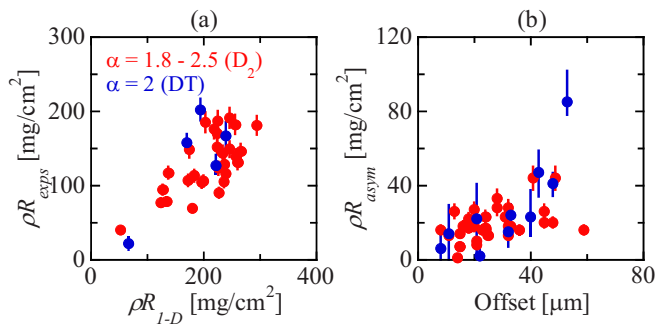


FIG. 6. (Color online) (a) Observed average  $\rho R$  as a function of 1D predicted  $\rho R$  for implosions with a capsule offset of less than  $40 \mu\text{m}$  to the target-chamber center. (b) Observed  $\rho R_{\text{asym}}$  as a function of capsule offset. These data sets are for low-adiabat DT [dark gray data points (blue online)] and  $\text{D}_2$  [light gray data points (red online)] implosions driven at various intensities. Similar performance relative to 1D and similar  $\rho R_{\text{asym}}$  as a function of capsule offset is observed for both DT and  $\text{D}_2$  implosions, indicating that the  $\rho R$  analysis of the KO-D spectrum is accurate.

DT implosions. From the simulated fits,  $\rho R$  values ranging from 25 to  $205 \text{ mg/cm}^2$  were inferred. The relatively low  $\rho R$ s for shots 43 070 and 43 945 are primarily due to a non-optimal designed laser-pulse shape that generated mistimed shocks. The performance of these implosions was also further degraded by the relatively large capsule offset of  $\sim 30\text{--}40 \mu\text{m}$  from target-chamber center. Although the offset was about the same for shot 49 035, the inferred  $\rho R$  is higher than for shots 43 070 and 43 945; a consequence of a better designed laser-pulse shape. The high  $\rho R$  value for shot 48 734 was achieved using the shock-ignition concept described in Refs. 19 and 20. The fact that the capsule was perfectly centered ( $11 \pm 15 \mu\text{m}$ ) resulted in a determined  $\rho R$  value close to the 1D simulated value of about  $200 \text{ mg/cm}^2$ . In addition, it is notable that the high-energy end points are at the theoretical maximum of 12.5 MeV, demonstrating that KO-Ds are produced in the outermost parts of the implosion and the plastic ablator has been burnt away entirely.

$\rho R$  data obtained for hydrodynamically equivalent cryogenic  $\text{D}_2$  implosions<sup>14</sup> were used to validate the  $\rho R$  analysis of the KO-D spectrum. As a well-established  $\rho R$  diagnostic method exists for cryogenic  $\text{D}_2$  implosions,<sup>21</sup> this comparison provides a good check of the analysis method described herein. The comparison is made in Figs. 6, which illustrates the experimental  $\rho R$  as a function of 1D predicted  $\rho R$  in (a) and the observed  $\rho R_{\text{asym}}$  as a function of capsule offset in (b) for low-adiabat DT and  $\text{D}_2$  implosions driven at various intensities. Both sets of data show similar behavior, demonstrating that the  $\rho R$  analysis of the KO-D spectrum is accurate.

#### IV. SUMMARY AND CONCLUSIONS

Through Monte Carlo modeling of a cryogenic DT implosion it has been demonstrated that the fuel  $\rho R$  in moderate  $\rho R$  ( $<200 \text{ mg/cm}^2$ ) cryogenic DT implosions at OMEGA can be determined accurately from the shape of the measured KO-D spectrum. The results from the Monte Carlo modeling of an implosion have provided a deeper understanding of the relationship between  $\rho R$ , implosion structure, and KO-D pro-

duction. In particular, it was established that the shape of the KO-D spectrum depends mainly on  $\rho R$ , and that effects of spatially varying density and temperature profiles play minor roles. Multidimensional features could, on the other hand, have an effect on the analysis and interpretation of the KO-D spectrum, as these effects would manifest themselves by slightly smearing out the high-energy peak for low fuel  $\rho R$  ( $<100 \text{ mg/cm}^2$ ). For higher  $\rho R$  ( $>150 \text{ mg/cm}^2$ ), these effects should be less prominent as high-mode nonuniformities would not significantly alter the shape of the KO-D spectrum. The  $\rho R$  analysis of the KO-D spectrum was also validated by comparing these results to  $\rho R$  data obtained for hydrodynamically equivalent cryogenic  $\text{D}_2$  implosions using a well-established  $\rho R$ -diagnostic method. The good agreement observed between the two analysis methods indicates that the KO-D analysis method described herein is accurate.

#### ACKNOWLEDGMENTS

The work described here was supported in part by U.S. DOE (Grant No. DE-FG03-03SF22691), LLE (Grant No. 412160-001G), LLNL (Grant No. B504974), and GA under the U.S. DOE (Grant No. DE-AC52-06NA27279).

- <sup>1</sup>T. R. Boehly, D. L. Brown, R. S. Craxton, R. L. Keck, J. P. Knauer, J. H. Kelly, T. J. Kessler, S. A. Kumpan, S. J. Bucks, S. A. Letzring, F. J. Marshall, R. L. McCrory, S. F. B. Morse, W. Seka, J. M. Soures, and C. P. Verdon, *Opt. Commun.* **133**, 495 (1997).
- <sup>2</sup>G. H. Miller, E. I. Moses, and C. R. Wuest, *Nucl. Fusion* **44**, S228 (2004).
- <sup>3</sup>P. W. McKenty, V. N. Goncharov, R. P. J. Town, S. Skupsky, R. Betti, and R. L. McCrory, *Phys. Plasmas* **8**, 2315 (2001).
- <sup>4</sup>J. A. Frenje, K. M. Green, D. G. Hicks, C. K. Li, F. H. Séguin, R. D. Petrasso, T. C. Sangster, T. W. Phillips, V. Yu. Glebov, D. D. Meyerhofer, S. Roberts, J. M. Soures, and C. Stoeckl, *Rev. Sci. Instrum.* **72**, 854 (2001).
- <sup>5</sup>J. A. Frenje, D. T. Casey, C. K. Li, J. R. Rygg, F. H. Séguin, R. D. Petrasso, V. Yu. Glebov, D. D. Meyerhofer, T. C. Sangster, S. Hatchett, S. Haan, C. Cerjan, O. Landen, M. Moran, P. Song, D. C. Wilson, and R. J. Leeper, *Rev. Sci. Instrum.* **79**, 10E502 (2008).
- <sup>6</sup>V. Yu. Glebov, D. D. Meyerhofer, T. C. Sangster, C. Stoeckl, S. Roberts, C. A. Barrera, J. R. Celeste, C. J. Cerjan, L. S. Dauffy, D. C. Eder, R. L. Griffith, S. W. Haan, B. A. Hammel, S. P. Hatchett, N. Izumi, J. R. Kimbrough, J. A. Koch, O. L. Landen, R. A. Lerche, B. J. MacGowan, M. J. Moran, E. W. Ng, T. W. Phillips, P. M. Song, R. Tommasini, B. K. Young, S. E. Caldwell, G. P. Grim, S. C. Evans, J. M. Mack, T. J. Sedillo, M. D. Wilke, D. C. Wilson, C. S. Young, D. Casey, J. A. Frenje, C. K. Li, R. D. Petrasso, F. H. Séguin, J. L. Bourgade, L. Disdier, M. Houry, I. Lantuejoul, O. Landoas, G. A. Chandler, G. W. Cooper, R. J. Leeper, R. E. Olson, C. L. Ruiz, M. A. Sweeney, S. P. Padalino, C. Horsfield, and B. A. Davis, *Rev. Sci. Instrum.* **77**, 10E715 (2006).
- <sup>7</sup>S. Kurebayashi, J. A. Frenje, F. H. Séguin, J. R. Rygg, C. K. Li, R. D. Petrasso, V. Yu. Glebov, J. A. Delettrez, T. C. Sangster, D. D. Meyerhofer, C. Stoeckl, J. M. Soures, P. A. Amendt, S. P. Hatchett, and R. E. Turner, *Phys. Plasmas* **12**, 032703 (2005).
- <sup>8</sup>S. Skupsky and S. Kacenjar, *J. Appl. Phys.* **52**, 2608 (1981).
- <sup>9</sup>S. Kacenjar, S. Skupsky, A. Entenberg, L. Goldman, and M. Richardson, *Phys. Rev. Lett.* **49**, 463 (1982).
- <sup>10</sup>C. K. Li, F. H. Séguin, D. G. Hicks, J. A. Frenje, K. M. Green, S. Kurebayashi, R. D. Petrasso, D. D. Meyerhofer, J. M. Soures, V. Yu. Glebov, R. L. Keck, P. B. Radha, S. Roberts, W. Seka, S. Skupsky, C. Stoeckl, and T. C. Sangster, *Phys. Plasmas* **8**, 4902 (2001).
- <sup>11</sup>F. H. Séguin, J. A. Frenje, C. K. Li, D. G. Hicks, S. Kurebayashi, J. R. Rygg, B.-E. Schwartz, R. D. Petrasso, S. Roberts, J. M. Soures, D. D. Meyerhofer, T. C. Sangster, J. P. Knauer, C. Sorce, V. Yu. Glebov, C. Stoeckl, T. W. Phillips, R. J. Leeper, K. Fletcher, and S. Padalino, *Rev. Sci. Instrum.* **74**, 975 (2003).
- <sup>12</sup>C. K. Li and R. D. Petrasso, *Phys. Rev. Lett.* **70**, 3059 (1993).

- <sup>13</sup>J. A. Frenje, C. K. Li, J. R. Rygg, F. H. Séguin, D. T. Casey, R. D. Petrasso, J. Delettrez, V. Yu. Glebov, T. C. Sangster, O. Landen, and S. Hatchett, *Phys. Plasmas* **16**, 022702 (2009).
- <sup>14</sup>T. C. Sangster, R. Betti, R. S. Craxton, J. A. Delettrez, D. H. Edgell, L. M. Elasky, V. Yu. Glebov, V. N. Goncharov, D. R. Harding, D. Jacobs-Perkins, R. Janezic, R. L. Keck, J. P. Knauer, S. J. Loucks, L. D. Lund, F. J. Marshall, R. L. McCrory, P. W. McKenty, D. D. Meyerhofer, P. B. Radha, S. P. Regan, W. Seka, W. T. Shmayda, S. Skupsky, V. A. Smalyuk, J. M. Soures, C. Stoeckl, B. Yaakobi, J. A. Frenje, C. K. Li, R. D. Petrasso, and F. H. Séguin, *Phys. Plasmas* **14**, 058101 (2007).
- <sup>15</sup>Y. Lin, T. J. Kessler, and G. N. Lawrence, *Opt. Lett.* **20**, 764 (1995).
- <sup>16</sup>T. R. Boehly, V. A. Smalyuk, D. D. Meyerhofer, J. P. Knauer, D. K. Bradley, R. S. Craxton, M. J. Guardalben, S. Skupsky, and T. J. Kessler, *J. Appl. Phys.* **85**, 3444 (1999).
- <sup>17</sup>S. Skupsky, R. W. Short, T. Kessler, R. S. Craxton, S. Letzring, and J. M. Soures, *J. Appl. Phys.* **66**, 3456 (1989).
- <sup>18</sup>J. Delettrez, *Can. J. Phys.* **64**, 932 (1986).
- <sup>19</sup>R. Betti, C. D. Zhou, K. S. Anderson, L. J. Perkins, W. Theobald, and A. A. Solodov, *Phys. Rev. Lett.* **98**, 155001 (2007).
- <sup>20</sup>W. Theobald, R. Betti, C. Stoeckl, K. S. Anderson, J. A. Delettrez, V. Yu. Glebov, V. N. Goncharov, F. J. Marshall, D. N. Maywar, R. L. McCrory, D. D. Meyerhofer, P. B. Radha, T. C. Sangster, W. Seka, D. Shvarts, V. A. Smalyuk, A. A. Solodov, B. Yaakobi, C. D. Zhou, J. A. Frenje, C. K. Li, F. H. Séguin, R. D. Petrasso, and L. J. Perkins, *Phys. Plasmas* **15**, 056306 (2008).
- <sup>21</sup>F. H. Séguin, C. K. Li, J. A. Frenje, S. Kurebayashi, R. D. Petrasso, F. J. Marshall, D. D. Meyerhofer, J. M. Soures, T. C. Sangster, C. Stoeckl, J. A. Delettrez, P. B. Radha, V. A. Smalyuk, and S. Roberts, *Phys. Plasmas* **9**, 3558 (2002).